A land-neutral expansion of Brazilian renewable fuel production - Supplementary Information

Luis Ramirez Camargo[1,2,3,*], Gabriel Castro[1,4], Katharina Gruber[1], Jessica Jewell[5], Michael Klingler[1,6], Olga Turkovska[1], Elisabeth Wetterlund[7,8] & Johannes Schmidt[1]

[1] *Institute for Sustainable Economic Development, University of Natural Resources and Life Science, Vienna, Austria*

[2] *Electric Vehicle and Energy Research Group (EVERGI), Mobility, Logistics and Automotive Technology Research Centre (MOBI), Department of Electrical Engineering and Energy Technology, Vrije Universiteit Brussel, Brussels, Belgium*

[3] *Flanders Make, 3001 Heverlee, Belgium*

[4] *Energy Planning Program, Graduate School of Engineering, Federal University of Rio de Janeiro, Rio de Janeiro, Brazil.*

[5] *Department of Space, Earth and Environment, Chalmers University of Technology*

[6] *Department of Geography, University of Innsbruck, Innsbruck, Austria*

[7] *Energy Engineering, Division of Energy Science, Luleå University of Technology, 971 87 Luleå, Sweden*

[8] *International Institute for Applied Systems Analysis (IIASA), A-2361 Laxenburg, Austria*

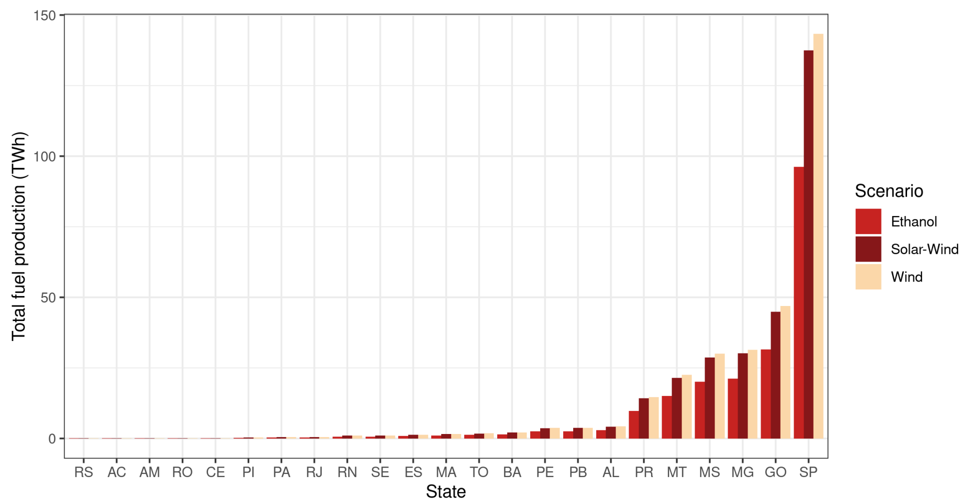

Supplementary Fig. 1. Share in total production of different states.

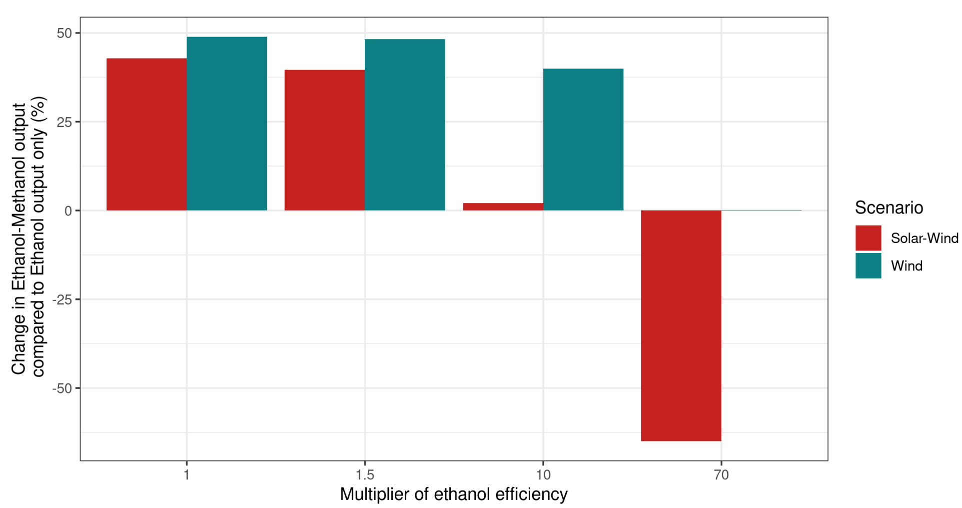

Supplementary Fig. 2. Change in output of the land-neutral methanol pathway in different ethanol land-use efficiency scenarios.

Supplementary Table 1. Technology assumptions.

Technology	CAPEX (€/kW)	OPEX (€/kW/a)	Lifetime (years)	Annualized cost (€/kW)	Efficiency	Source
PV						Cost projection for
Low	290	8.8	20	35	-	2020(high) and 2030(low)
High	430	6,4	20	53		are taken from[1]
Wind						Cost projection for 2020(high) and 2030(low)
Low	1,040	12	20	118	-	are taken from[2].
High	1,120	14	20	128		OPEX are taken from[3]
Electrolyzers						The selected values are a conservative summary
Low	250	5.0	20	30	63%	of the references provided
Mid	500	10.0	20	60		in Supplementary Table 2.
High	780	15.7	20	95	69%	OPEX and efficiency from[3]
Methanol synthesis	300	12	20	43	83% (from H_2)	[4]
	CAPEX (€/t)		**Lifetime (years)**	**Annualized cost (€/t)**		
H_2 - Storage						
Low	7,020		20	715	100%	[5]
High	376,400		20	38,300		
CO_2 - Storage						
Low	0.135		20	0.014	100%	[6]
High	20		20	2		[7]
Battery						Low and high opex and capex costs represent costs
Low	117	2.7	15	16	90%	taken from[1] for 2020
High	250	3.9	15	33		and 2030, respectively.

Supplementary Table 2. Electrolyzer costs reported in the literature.

Electrolyzer type [year]	Price (range) [USD/kW]	Reference
Alkaline [2020]	571-1,268	[8]
PEM [2020]	385-2,068	[8]
PEM [2020]	800	[9]
PEM [2030]	300	[9]
Generic [2020]	500-950	[10]
Generic [2030]	400-950	[10]
Generic [2040/current Chinese low cost]	200	[11]

Supplementary Table 3. CO_2 capture costs from ethanol production reported in the literature.

Reference Year	Price (range) [EUR/tCO_2]	Reference
2020	<10	[12]
2017	Close to 0	[13]
2017	<8	[14]

Supplementary Note 1. Results - Sensitivity analysis

Here, we assess the sensitivity of model results to weather years (Supplementary Fig. 3) and storage and wind power costs (Supplementary Fig. 4). We ran the model for three different weather year configurations: first, for our reference year 2016. Average PV electricity generation in this year is closest to the average annual PV electricity generation in the period 1999-2018. Second we simulated the years with the lowest annual wind and PV generation, and the ones with the highest annual wind and PV generation. For these runs, the lowest/highest generation years were defined by the individual minimum or maximum production years in the whole time series of 20 years (1999-2018) per location. Therefore, the optimization model was run for three different years at all locations: for 2016, for the year with the lowest and for the year with the highest generation at that location. This is, of course, a rather extreme assumption, as the best years are not uniform among regions. In this way, however, we were able to cover the most extreme impacts of climate on results.

Although we took a rather extreme approach, the impacts on both of our key performance indicators, i.e., land used by renewables and final costs, were minor. Deviations were below +/-5% for costs, and below +/-7% for the land-used by VRES. We, therefore, conclude that the choice of the weather year has a minor impact on the overall outcome.

The impact of different storage and wind power cost assumptions (see Supplementary Table 1) on results are also small (Supplementary Fig. 4). First, battery storage is not used in any of the scenarios, independent of cost assumptions. Second, the share of CO_2 and H_2 storage costs in total costs is insignificant compared to the costs of electrolyzers and VRES. This is implied by the very low costs of CO_2-storage, and the very small levels of H_2 storage deployed. Third, our wind power cost assumptions do not vary significantly between sensitivity runs, as we consider it to be a mature technology. The minor changes in costs do consequently not affect output strongly.

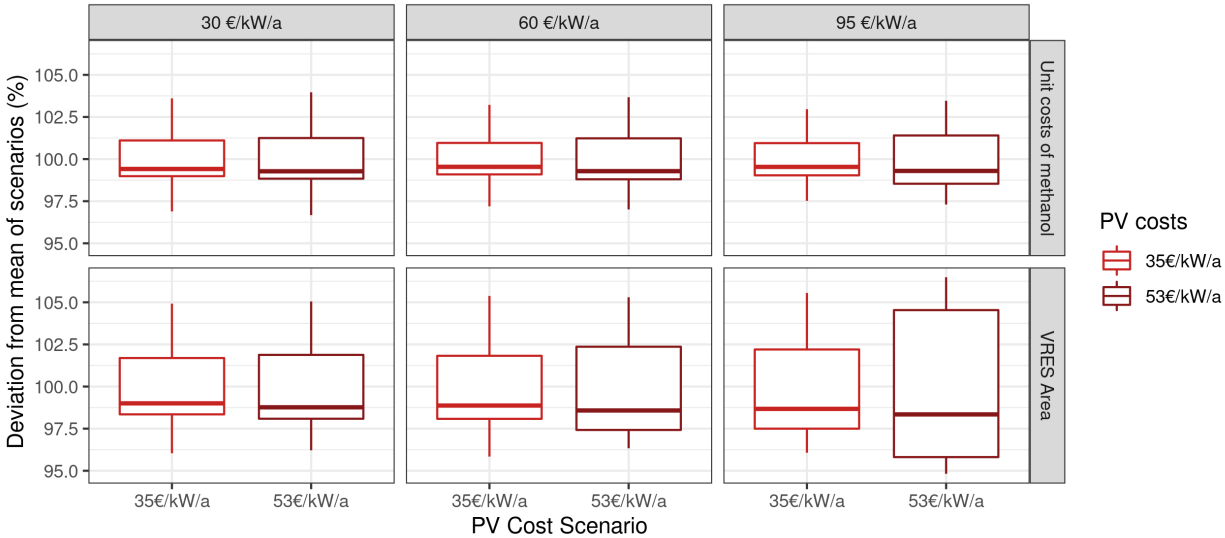

Supplementary Fig. 3. The impact of different weather years on VRES area and costs for different electrolyzer cost assumptions From left to right: 30, 60 and 95 EUR/kW/a annualized electrolyzer cost.

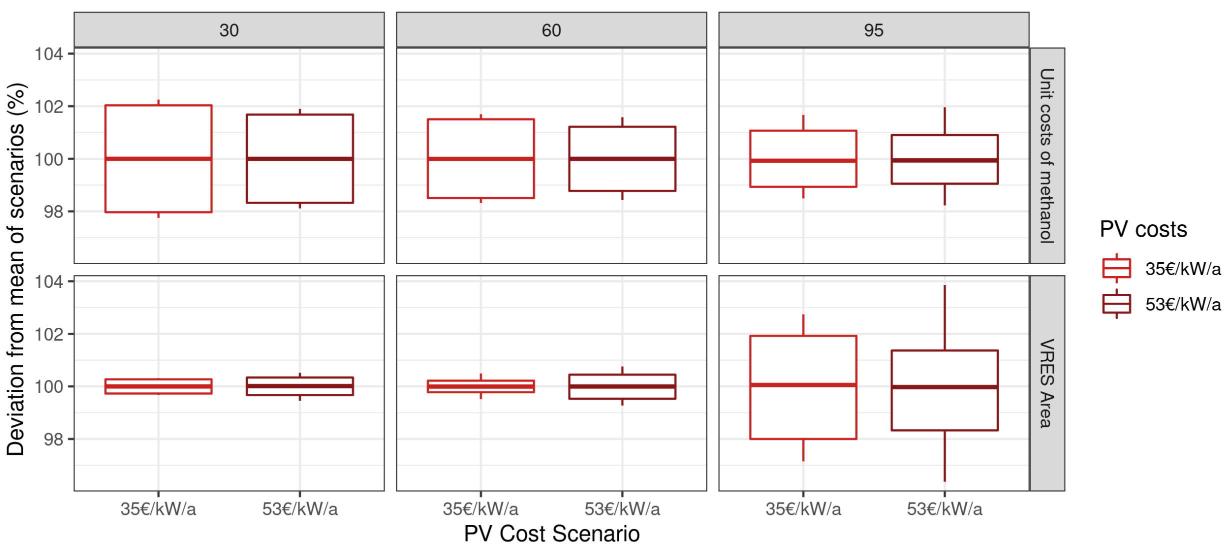

Supplementary Fig. 4. The impact of storage and wind power cost assumptions on land-use and costs for different electrolyzer cost assumptions. From left to right: 30, 60 and 95 EUR/kW/a annualized electrolyzer costs.

Supplementary Note 2. Results - CO_2 emissions and abatement costs

We calculated CO_2 abatement costs by assuming that renewable methanol substitutes methanol produced from fossil natural gas at an emission factor of 335.8tCO_2/GWh[15]. We assumed a cost of methanol produced from fossil gas at 0.04€/kWh[16], sorted all locations by production costs from lowest to highest, and calculated the potential abated emissions by the sum of the production times the emission factor. Abatement costs were calculated as the difference of renewable production costs and fossil production costs divided by the emission factor. These are presented in Supplementary Fig. 5.

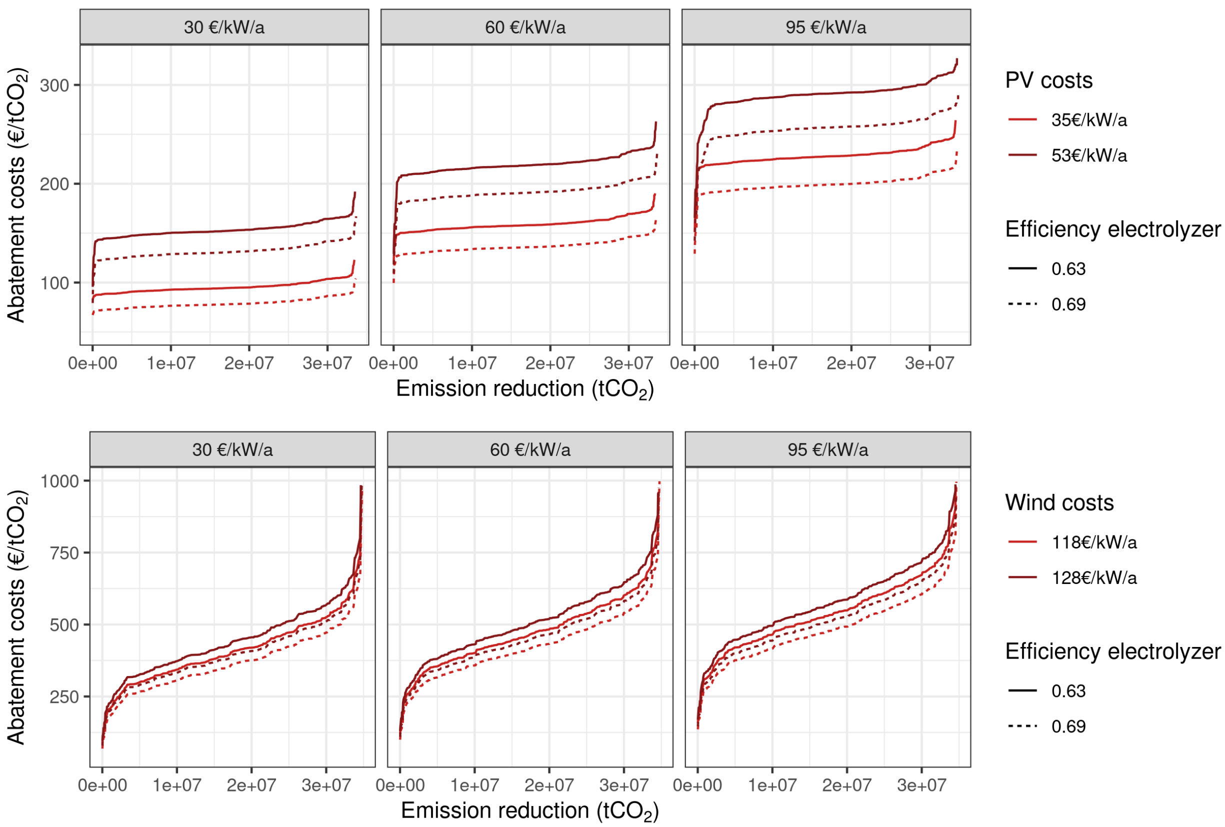

Supplementary Fig. 5. CO_2 abatement cost curves. Upper: solar-wind scenario. Lower: wind scenario. From left to right: annualized electrolyzer cost assumptions.

Supplementary Note 3. Results - Explaining costs of renewables

Supplementary Fig. 6 shows how the full load hours of wind and PV impact the methanol production costs for the solar-wind scenario. We also developed a simple regression model, which tests the influence of input parameters on the methanol production costs:

$$costs_{methanol} = \beta_0 + \beta_1 PV_{avg} + \beta_2 Wind_{high-cap} + \beta_3 length_{season}$$

In particular, we included the full load hours of PV generation PV_{avg} on cost, and a dummy variable $Wind_{high-cap}$ which is set to 1 if the capacity factor of wind power is above 0.3 at the respective location. We did not use wind capacity factors directly, as the relation between wind power full capacity factors and methanol cost is highly non-linear. However, for estimating a non-linear function such as a high order polynomial the number of data points is too low. We therefore opted to include the dummy variable instead. We also ran alternative specifications of the model in terms of representing wind resources, which changed results quantitatively, but not qualitatively. Additionally, we included the variable $length_{season}$ that indicates if CO_2 supply is stretched out during the whole year or if it is concentrated in a few months. The variable measures the length of the period between the maximum and the minimum of the time series $cumsum(CO2 - stream - mean(CO2 - stream))$. To determine parameters of the regression model, we used the solar-wind scenario with average input cost assumptions. Using other scenarios in the regression changes the results quantitatively, i.e. coefficients are changed, but not qualitatively. The results are shown in Supplementary Table 4.

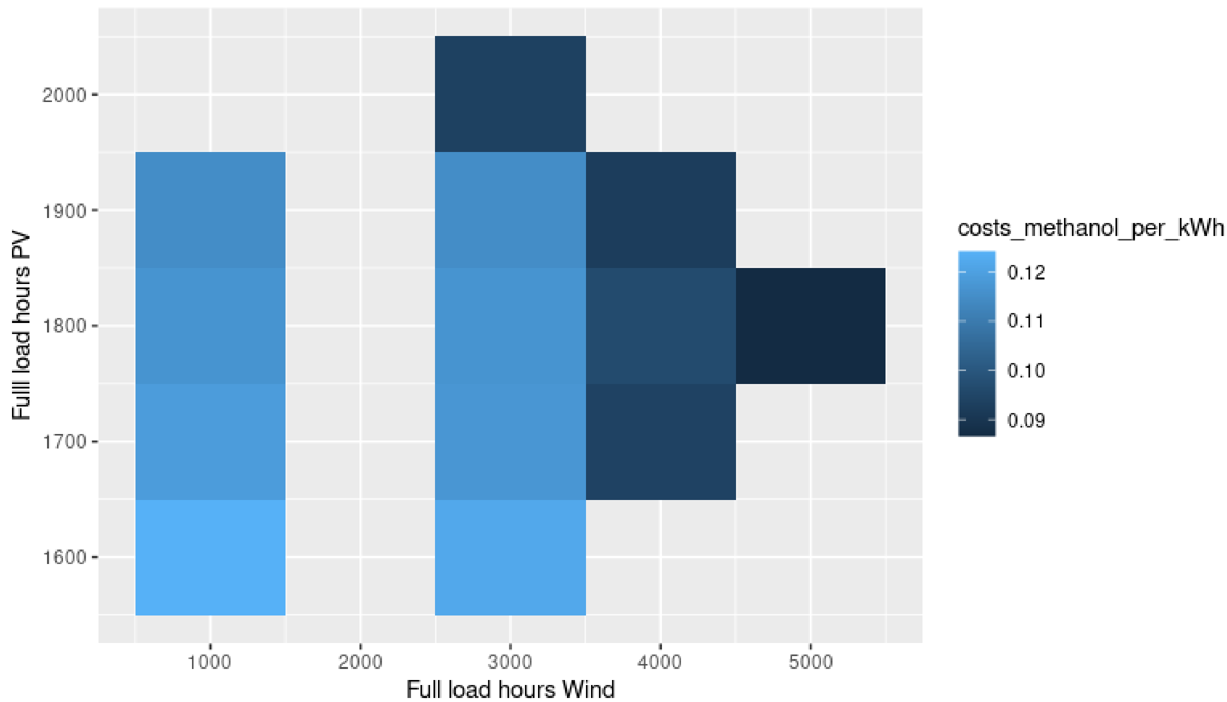

Supplementary Fig. 6. Full load hours of wind and PV and methanol production costs in the most expensive solar-wind scenario.

Supplementary Table 4. Regression model of model input parameters on costs of methanol production (€/kWh). We used the solar-wind scenario with the highest input cost assumptions.

	Costs methanol per kWh			
Predictors	***Estimates***	***Std-Error***	***t-value***	***p***
(Intercept)	**0.14**	**0.0024**	**60.36**	**$<$0.001**
PV_{avg}	**-0.2104**	**0.0111**	**-18.86**	**$<$0.001**
$wind_{high-cap}$	**-0.0042**	**0.0005**	**-8.94**	**$<$0.001**
$length_{season}$	**-0.0004**	**0.0000**	**-15.23**	**$<$0.001**
Observations	**339**			
R^2 / R^2 adjusted	**0.65 / 0.64**			

Supplementary Note 4. Methods - Optimization model equations

The objective function for the cost minimization (eq. 1) sums up capacities times cost per unit of VRES generation, i.e. PV and Wind power, ($x\_vresBuild, resCost$), the cost per unit of storage systems ($x\_storageSize, storageCost$), the cost per unit of electrolyzers ($x\_electrolyzerSize$, $electrolyzerCost$) and the cost per unit of methanol synthesis unit ($x\_methanolSynthesisSize$, $methanolSynthesisCost$). The subindex $tech$ denotes technology which can be either photovoltaic or wind power, $subtech$ denotes the sub-technology classification that can be IEC I or IEC II for wind turbines (see Supplementary Note 6 for details) and c denotes the type of storage that can be either electricity, H_2 or CO_2 (An overview of the sets, parameters and variables used is provided in supplementary tables 5, 6 and 7 respectively).

$$\begin{aligned} x\_cost = \sum_{tech}\sum_{subtech} & x\_vresBuild_{(tech,subtech)} \times vresCost_{(tech,subtech)} \\ & + \sum_{c} x\_storageSize_c \times storageCost_c \\ & + x\_electrolyzerSize \times electrolyzerCost \\ & + x\_methanolSynthesisSize \times methanolSynthesisCost \end{aligned} \quad (1)$$

The VRES generation per time step $x\_vresGeneration_t$ is balanced with the installed capacity ($x\_vresBuild_{(tech,subtech)}$) times the production profile ($vresOutput_{(t,tech,subtech)}$) as shown in eq. 2. VRES generation is also balanced with instantaneously used power ($x\_vresPowerToUse_t$), inflows to battery storage ($x\_storageInput_{(t,"electricity")}$) and curtailment ($x\_vresCurtail_t$) as presented in eq. 3.

$$\begin{aligned} x\_vresGeneration_t = \sum_{t}\sum_{tech}\sum_{subtech} & x\_vresBuild_{(tech,subtech)} \\ & \times vresOutput_{(t,tech,subtech)} \quad \forall t \end{aligned} \quad (2)$$

$$\begin{aligned} x\_vresGeneration_t = x\_vresPowerToUse_t & + x\_storageInput_{(t,"electricity")} \\ & + x\_vresCurtail_t \quad \forall t \end{aligned} \quad (3)$$

The speed of charging ($x\_storageInput_{(t,c)}$) or discharging ($x\_storageOutput_{(t,c)}$) storage systems is limited by the installed capacity ($x\_storageSize_c$) times a charging speed limit

($storageCapacityLimitPercentage_c$) (eq. 4 and 5).

$$x\_storageInput_{(t,c)} \leq x\_storageSize_c \times storageCapacityLimitPercentage_c \quad \forall t, c \tag{4}$$

$$x\_storageOutput_{(t,c)} \leq x\_storageSize_c \times storageCapacityLimitPercentage_c \quad \forall t, c \tag{5}$$

Equation 6 shows how the state of charge ($x\_soc_{(t,c)}$) is balanced with the state of charge one time step before, accounting for temporal storage losses, with charging energy ($x\_storageInput_{(t,c)}$), considering charging losses $storageEffcharg_c$, and discharging energy $x\_storageOutput_{(t,c)}$.

$$\begin{aligned} x\_soc_{(t,c)} = (x\_soc_{(t-1,c)} \times (1 - storageLoss_c)) + (storageEffcharg_c \\ \times x\_storageInput_{(t,c)}) - x\_storageOutput_{(t,c)} \quad \forall t, c \end{aligned} \tag{6}$$

The sum of the electricity used to produce H_2 in this time step ($electricityGenerationH2_t$) is balanced with the sum of instantaneously used VRES electricity and the output of the electrical storage (eq. 7).

$$electricityGenerationH2_t = x\_vresPowerToUse_t + x\_storageOutput_{(t,electricity)} \quad \forall t \tag{7}$$

Moreover, the amount of CO_2 that is used for the production of methanol in any particular time step (eq. 8) is equal to the sum of the CO_2 stream from the ethanol production ($co2Stream_t$) and the output of the CO_2 storage ($x\_storageOutput_{(t,"CO_2")}$) minus the CO_2 stored ($x\_storageInput_{(t,"CO_2")}$).

$$\begin{aligned} x\_co2ToMethanol_t = co2Stream_t + x\_storageOutput_{(t,"CO_2")} \\ - x\_storageInput_{(t,"CO_2")} \quad \forall t \end{aligned} \tag{8}$$

The amount of H_2 (x_h2_t) is determined in two different equations (eq. 9 and eq. 10). It is equal to the electricity use of the electrolyzer ($electricityGenerationH2t$) multiplied by the efficiency of the electrolyzer ($h2Eff$). It's level is limited by the electrolyzer size ($x\_electrtolyzerSize$) multiplied by its efficiency.

$$x\_h2_t = electricityGenerationH2_t \times h2Eff \quad \forall t \tag{9}$$

$$x\_h2_t \leq x\_electrolyzerSize \times h2Eff \quad \forall t \tag{10}$$

Similarly the amount of methanol in a particular time step ($x\_methanol_t$) is limited on the one side (eq. 11) by the size of the methanol synthesis installation ($x\_methanolSynthesisSize$) and on the other side (eq. 12) by the methanol synthesis efficiency ($methanolSynthesisEff$) multiplied by the amount of H_2 that can be transformed into methanol in that time step ($x\_h2ToMethanol_t$). The latter is also equal to the sum of H_2 produced in that time step (x_h2_t) and the difference between charge ($x\_storageInput_{(t,"h_2")}$) and discharge ($x\_storageOutput_{(t,"h_2")}$) of the H_2 storage (eq. 13).

$$x\_methanol_t \leq x\_methanolSynthesisSize \quad \forall t \tag{11}$$

$$x\_h2ToMethanol_t \times methanolSynthesisEff = x\_methanol_t \quad \forall t \tag{12}$$

$$x\_h2ToMethanol_t = x\_h2_t + x\_storageOutput_{(t,"h_2")} - x\_storageInput_{(t,"h_2")} \quad \forall t \tag{13}$$

Finally, eq. 14 presents the restriction for the transformation of CO_2 into methanol ($x\_co2ToMethanol_t$). It depends on the amount of H_2 that can be transformed into methanol at a particular time step and the proportion between CO_2 and H_2 for each Methanol unit ($balanceCO2H2$).

$$x\_h2ToMethanol_t \times balanceCO2H2 = x\_co2ToMethanol_t \quad \forall t \tag{14}$$

Supplementary Table 5. Optimization model sets.

Name	Symbol	Unit	Elements
Time steps	*t*	*h*	t_1,t_2,...,t_n
commodity	*c*	-	*Electricity*,CO_2, H_2
technology	*tech*	-	*pv,wind*
Sub-technology	*subtech*	-	*IECI, IECII (for wind turbines)*

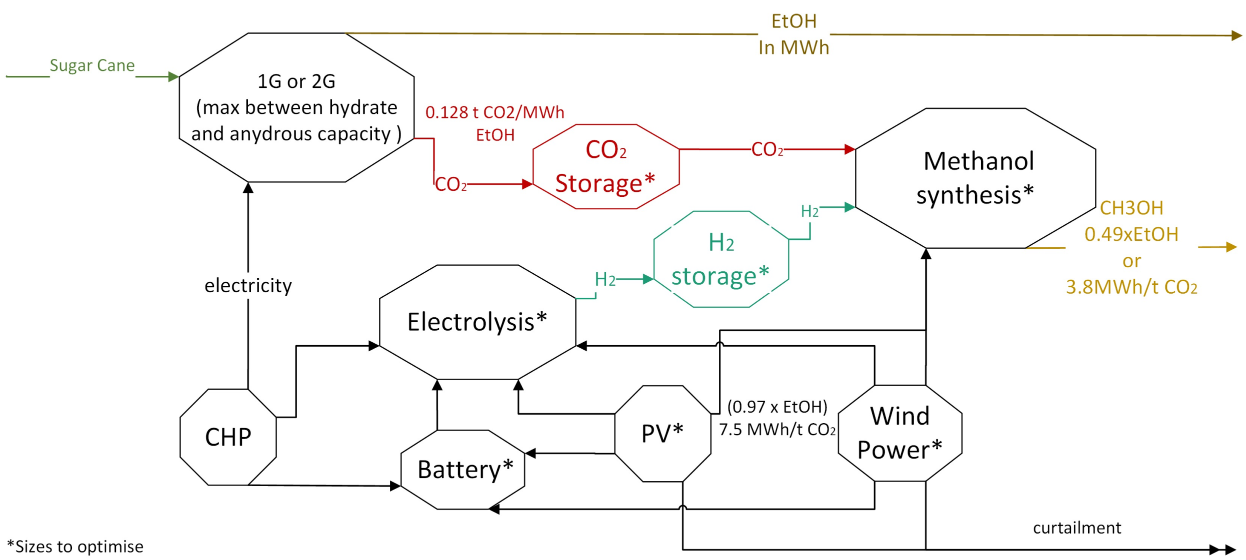

Fig. 7. Schematic presentation of the model for each sugarcane to ethanol and methanol installation.

Supplementary Table 6. Optimization model parameters.

	Name	Symbol	Unit	Value
Time Series	Electric energy generation of VRES	vresOutput(t, tech, subtech)	GWh	Variate per time step and location (see methods section)
	CO_2 generated in the ethanol production	co2Streamt	t	
Costs	Cost of VRES technologies	vresCost(tech, subtech)	EUR/GW	See Supplementary Table 1.
	Cost of the electrolyzer	electrolyzerCost	EUR/GW	See Supplementary Table 1.
	Cost of the methanol synthesis system	methanolSynthesisCost	EUR/GWh	See Supplementary Table 1.
	Cost of storage	storageCostc	EUR/GWh and EUR/t	See Supplementary Table 1.
Efficiencies and commodities transformation balances	Efficiency of storage	storageEffchargc	%	See Supplementary Table 1.
	Losses of the storage system from one period to the next	storageLosst	%	electricity=0.1 CO_2=0 H_2=0
	Charge and discharge capacity of storage systems	storageCapacityLimitPercentagec	%	electricity=40 CO_2=20 H_2=20
	Balance between CO_2 and H_2 for each Methanol unit	balanceCO2H2	-	7.268519[4]
	Electrolyzer efficiency	h2Eff	kt/GWh (LHV)	See Supplementary Table 1.
	Methanol synthesis efficiency	methanolSynthesisEff	GWh/kt (LHV)	28.21[4]

Supplementary Table 7. Optimization model variables.

Name	**Symbol**	**Unit**
Total annualized system costs	x_cost	EUR
Total VRES generation	$x\_vresGeneration_t$	GWh
VRES installed capacity	$x\_vresBuild_{(tech,subtech)}$	GW
VRES electricity with immediate use	$x\_vresPowerToUse_t$	GWh
VRES electricity to store	$x\_vresToStorage_t$	GWh
VRES electricity to curtail	$x\_vresCurtail_t$	GWh
Storage system input	$x\_storageInput_{(t,c)}$	GWh or kt
State of charge of storage	$x\_soc_{(t,c)}$	GWh or kt
Storage system output	$x\_storageOutput_{(t,c)}$	GWh or kt
Storage system size	$x\_storageSize_c$	GWh or kt
Electrolyzer size	$x\_electrolyzerSize$	GW
Hydrogen produced	x_h2_t	GWh
Methanol Synthesis	$x\_methanolSynthesisSize$	GW
Methanol produced	$x\_methanol_t$	GWh
Electricity to produce H_2	$x\_electricityGenerationH2_t$	GWh
CO_2 to methanol	$x\_co2ToMethanol$	kt
H_2 to methanol	$x\_h2ToMethanol$	kt

Supplementary Note 5. Methods - Sugarcane facility data set

The Brazilian sugarcane ethanol industry is highly dynamic and dependent on local regulation, national and international markets. While there are companies that have been in the market for decades, ethanol-producing installations are commissioned, re-commissioned and closed regularly. Furthermore, the production in each installation is not only conditioned by the seasonality of the sugar cane and weather, but also by the changes in prices of fuels and sugar at the national and international level. The consequence is that there is no single or consolidated data set on ethanol generation plants in Brazil. Previous studies modeling Brazilian ethanol production avoided the problem by either denying it or working only with data of one single exemplary installation. However, the spatial location and the time series of CO_2 emissions for each ethanol plant are necessary to properly account for the integration of variable renewables in methanol production.

The three official sources for data of the Brazilian ethanol industry are the Energy research company (EPE- Empresa de Pesquisa Energética), the National Agency of Petroleum, Natural Gas and Biofuels (ANP-Agência Nacional Do Petróleo, Gás Natural e Biocombustíveis) and the Ministry of Agriculture (MAPA-Ministério da Agricultura, Pecuária e Abastecimento). These provide lists of installations but differ not only in the number of reported installations but also in the provided attributes or the values of attributes. We, therefore, constructed a synthetic data set that consolidates the data of the available sources. The EPE data set (381 installations) was used as a basis since it is the only one providing geographic coordinates for the installations. We confirmed the existence and installed capacity of the installations using the ANP data set (360 installations including not only sugar cane but also corn, rice and soy), which was matched in a semi-automatic fashion supported by similarity ratings on the names of the installations as well as by proximity assessments. The ANP data set provides addresses, which were georeferenced for that purpose. The existence of the installations was corroborated again using the MAPA data set and in case of doubt about the match of the installation between the three previous data sets, a manual online search was conducted for those cases. Details can be found in the github repository.

The synthetic data set includes 339 installations that run mainly on sugarcane. Based on

ANP, the installations have average daily generation capacities of 365 m^3 and 676 m^3 for anhydrous ethanol and hydrated ethanol, respectively. There are however large differences between installations and the largest ones reach processing capacities of 1,710 m^3/day of anhydrous ethanol and 2,800 m^3/day of hydrated ethanol. Hydrated ethanol is composed of approximately 96% ethanol and 4% water while Anhydrous ethanol contains at least 99.7% ethanol. The distillation process is common to both types of ethanol but the production of anhydrous ethanol requires an additional dehydration step to reduce the water content[17]. Considering this, we rated the processing capacity of each installation as the maximum value of the capacities for hydrous and anhydrous ethanol.

Apart from the location, the daily processing capacities, the state, the municipality and the type of biomass processed by each plant, there is not much public official information available on the installations. Based on Empresa de Pesquisa Energética[18], we could confirm that only two of the installations have second-generation ethanol production and identify these installations in the data set. To approximate the sugar cane harvesting area of each installation, we relied on statistics of the Companhia Nacional de Abastecimento (CONAB) for each state. We calculated the average of harvested area for the last five years and distributed it by installation based on the share of ethanol processing capacity of each installation when compared to the sum of processing capacity of all installations in a particular state. The majority of sugarcane to ethanol production in Brazil is concentrated in the state of São Paulo, which has a number of installations and installed ethanol processing capacities larger than the next six states combined (Supplementary Fig. 1). From 339 installations in the consolidated data set, 145 are located in this state, with a total processing capacity of 107,348 m^3 ethanol per day. This is followed by the state of Goiás, which hosts 36 installations, but is also home of several of the largest installations in the country with processing capacities of up to 2,800 m^3 ethanol per day. These states are followed in number of installations by the neighbouring states of Minas Gerais, Paraná and Mato Grosso do Sul, which have installed capacities for ethanol production of 34,210, 21,882, 13,460 and 22,385 m^3/day, respectively.

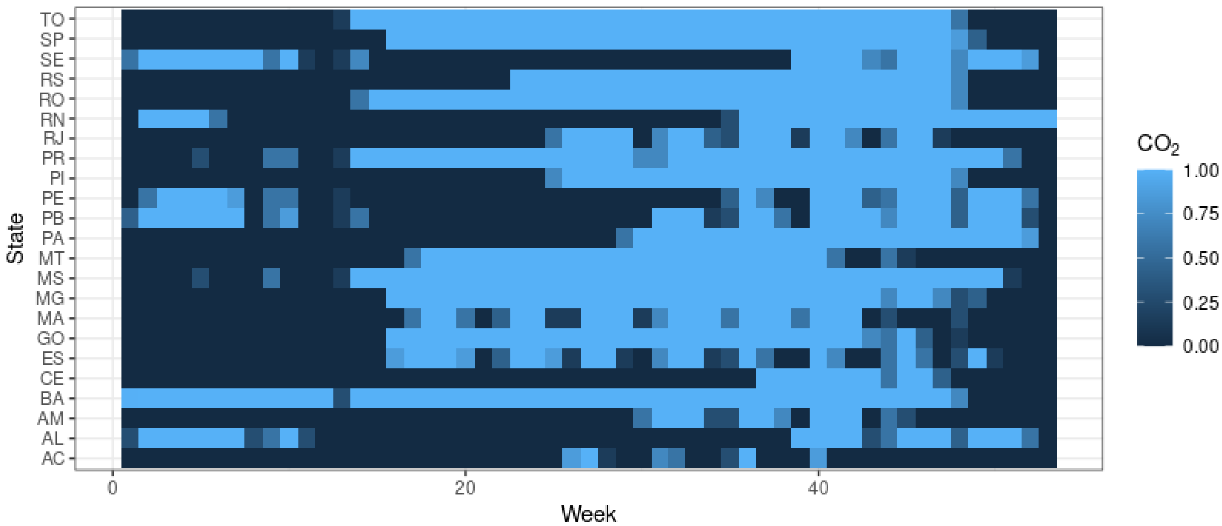

Supplementary Fig. 8. Heatmap of CO_2 streams from sugarcane fermentation for all states, normalized by maximum production per state.

Supplementary Note 6. Methods - VRES installation capacity factors and footprints

Supplementary Fig. 9 and 10 present the average weekly capacity factors for solar PV and wind power installation at all locations.

The tables in this note include the results of the assessment of Brazilian photovoltaic installation footprints (Supplementary Table 8), the corresponding descriptive statistics (Supplementary Table 9), and the footprints of installations reported in the scientific literature (Supplementary Table 10). In Brazil, we measured seven locations. For Apodi, however, different information on total installed capacity was found[19] and therefore this installation is included twice in the table. The footprints are in a similar range to installations reported in the scientific literature. For the panels only, values of 7.1 to 14 m²/kWp were found in the literature, while for the impact of total systems, depending on the type of system, land-use values between 15.4 and 36.4 m²/kWp, except for one extreme case of 50 m²/kWp, were found.

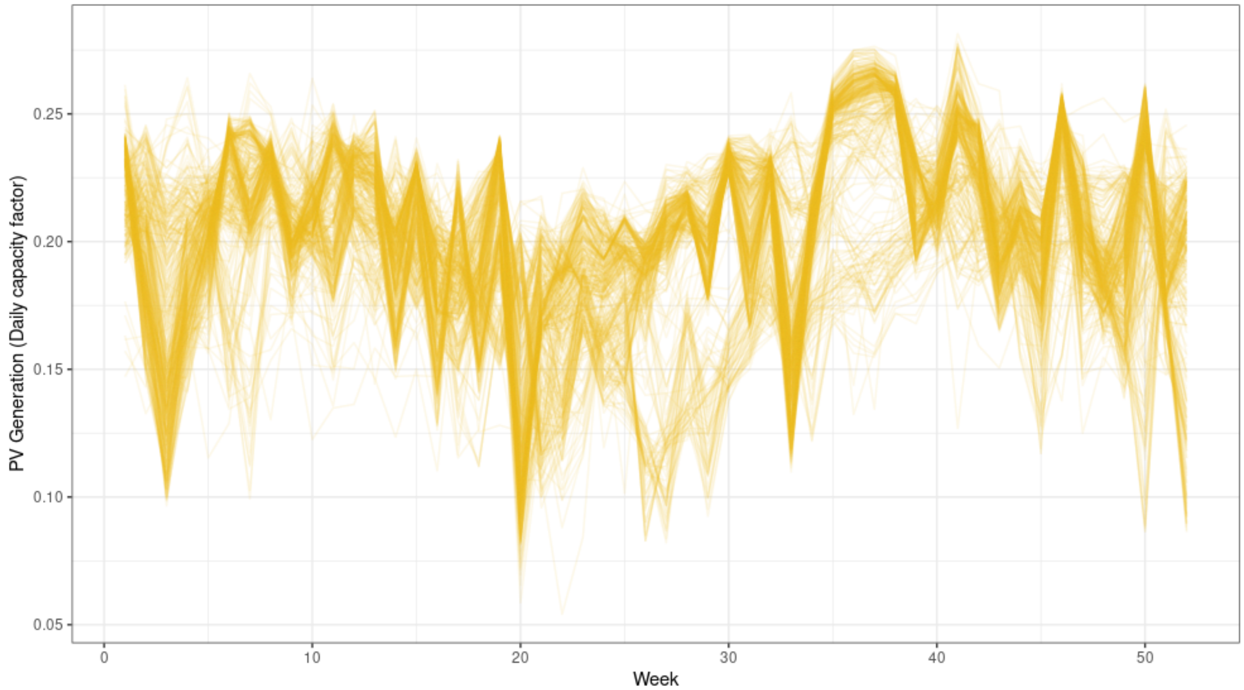

Supplementary Fig. 9. Average weekly capacity factor of solar PV installations at all locations.

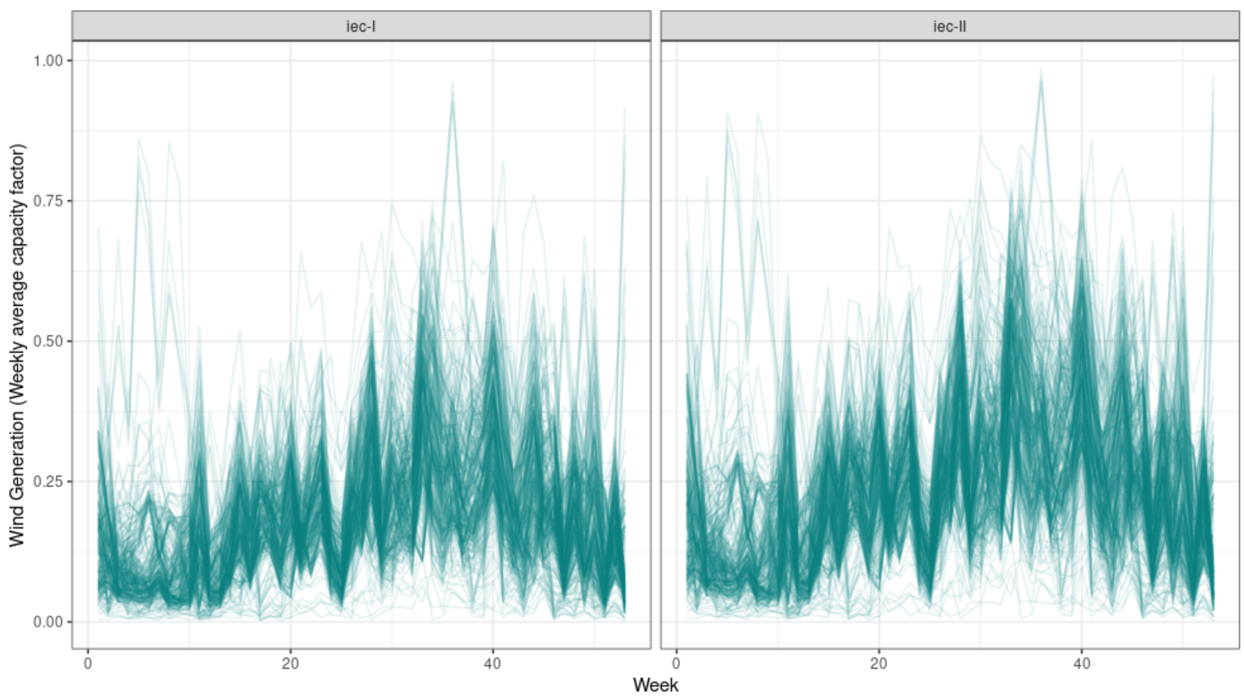

Supplementary Fig. 10. Wind power generation time series at all locations. Left: time series for turbine type 1, right: time series for turbine type 2.

Supplementary Table 8. Footprints of photovoltaic installations at seven locations in Brazil.

Plant	State	Capacity (MW)	Year of installation	lon	lat	Area (m^2) with spacing	Area (m^2) without spacing	m^2/kWp with spacing	m^2/kWp without spacing
Nova Aurora	SC	3.07	2013	-48.97	-28.45	44490	40625	14.5	13.2
Tanquinho	SP	1.08	2012	-47.04	-22.88	18964	13642	17.5	12.6
Apodi I - IV	CE	132	2018	-37.79	-5.04	4050000	1178998	30.7	8.9
Apodi I - IV	CE	162	2018	-37.79	-5.04	4050000	1178998	25.0	7.3
Floresta I - III	RN	86	2017	-36.91	-4.96	2900000	750037.5	33.7	8.7
Guimarania 1 + 2	MG	62	2018	-46.67	-18.82	1807653	819383.5	29.2	13.2
Assú V	RN	30	2017	-37.03	-5.55	873546	306397	29.1	10.2
Guaimbé 1 - 5	SP	150	2018	-49.87	-21.89	2250000	1801319	15.0	12.0

Supplementary Table 9. Descriptive statistics of footprints of photovoltaic installations in Brazil.

Quantile	m^2/kWp with spacing	m^2/kWp without spacing
0	14.50	7.28
25%	21.26	8.83
50%	29.14	9.57
75%	29.15	11.56
100%	33.72	13.22
mean	24.3	10.8

Supplementary Table 10. Footprints of photovoltaic installations reported in the literature.

Given unit	Land requirement [m²/kWp]	System type	Source
	with spacing		
35 W/m²	28.6	land use	20
65 W/m²	15.4	25° tilt south panel, USA	21
48 W/m²	20.8	1-axis tracking panel, USA	21
20 W/m²	50	2-axis tracking panel, USA	21
7.5 acres/MWac	30.4	total LU large PV, fixed	22
8.3 acres/MWac	33.6	total LU large PV, 1-axis	22
8.1 acres/MWac	32.8	total LU large PV, 2-axis CPV	22
5.8 acres/MWac	23.5	direct LU large PV, fixed	22
9.0 acres/MWac	36.4	direct LU large PV, 1-axis	22
6.1 acres/MWac	24.7	direct LU large PV, 2-axis CPV	22
	Without spacing		
1.4 ha/MWp	14	area	23
7.1 m²/kWp	7.1	panel	24
135 W/m²	7.3	flat panel (rooftop), USA	21
118 W/m²	8.5	10° tilt south panel (rooftop), USA	21

References

1. Vartiainen, E., Masson, G., Breyer, C., Moser, D. & Medina, E. R. Impact of weighted average cost of capital, capital expenditure, and other parameters on future utility-scale pv levelised cost of electricity. *Progress in Photovoltaics: Research and Applications* **28**, 439–453 (2020).

2. Danish-Energy-Agency & Energinet. Technology data -energy plants for electricity and district heating generation. Tech. Rep., Danish Energy Agency (2016). URL https://ens.dk/sites/ens.dk/files/Analyser/technology_data_catalogue_for_el_and_dh.pdf. [Online; accessed 2020-12-17].

3. Armijo, J. & Philibert, C. Flexible production of green hydrogen and ammonia from variable solar and wind energy: Case study of chile and argentina. *International Journal of Hydrogen Energy* **45**, 1541–1558 (2020).

4. Hannula, I. Co-production of synthetic fuels and district heat from biomass residues, carbon dioxide and electricity: Performance and cost analysis. *Biomass and Bioenergy* **74**, 26–46 (2015).

5. Kruck, O., Crotogino, F., Prelicz, R. & Rudolph, T. Overview on all known underground storage technologies for hydrogen. Tech. Rep., HyUnder Project (2013).

6. ZEP. The costs of co_2 storage. Tech. Rep., European Technology Platform for Zero Emission Fossil Fuel Power Plants (2011). URL https://zeroemissionsplatform.eu/wp-content/uploads/CO2-Storage-Report.pdf. [Online; accessed 2020-11-15].

7. Rubin, E. S., Davison, J. E. & Herzog, H. J. The cost of co_2 capture and storage. *International Journal of Greenhouse Gas Control* **40**, 378–400 (2015).

8. Christensen, A. Assessment of hydrogen production costs from electrolysis: United states and europe. *Internation Council on Clean Transportation* 73 (2020).

9. Mallapragada, D. S., Gençer, E., Insinger, P., Keith, D. W. & O'Sullivan, F. M. Can industrial-scale solar hydrogen supplied from commodity technologies be cost competitive by 2030? *Cell Reports Physical Science* **1**, 100174 (2020).

10. Brändle, G., Schulte, S. & Schönfisch, M. Estimating long-term global supply costs for low-carbon hydrogen. *Institute of Energy Economics at the University of Cologne Working Paper* (2020).

11. IRENA. *Hydrogen: A renewable energy perspective* (International Renewable Energy Agency, 2019).

12. Powerfuels, G. A. Carbon sources for powerfuels production. Tech. Rep., Deutsche Energie-Agentur GmbH (2020). URL https://www.powerfuels.org/fileadmin/powerfuels.org/Dokumente/GAP_Discussion_Paper_Carbon_Sources_for_Powerfuels_Production.pdf. [Online; accessed 2020-12-07].

13. Pilorgé, H. *et al.* Cost analysis of carbon capture and sequestration of process emissions from the u.s. industrial sector. *Environmental Science & Technology* **54**, 7524–7532 (2020).

14. CO_2-EOR. Capturing and utilizing co_2 from ethanol: Adding economic value and jobs to rural economies and communities while reducing emissions. Tech. Rep., State CO_2-EOR Deployment Work Group (2017). URL http://www.kgs.ku.edu/PRS/ICKan/2018/March/WhitePaper_EthanolCO2Capture_Dec2017_Final2.pdf. [Online; accessed 2020-12-07].

15. Prussi, M., De Prada, L., Edwards, R., Padella, M. & Yugo, M. *JEC well-to-tank report V5: JEC well to wheels analysis : well to wheels analysis of future automotive fuels and powertrains in the European context.* (Joint Research Centre (European Commission), LU, 2020). URL https://data.europa.eu/doi/10.2760/100379. [Online; accessed 2020-12-13].

16. Methanex-Corporation. Methanol pricing (2020). URL https://www.methanex.com/our-business/pricing. [Online; accessed 2020-12-11].

17. Holler Branco, J. E., Holler Branco, D., Aguiar, d. E. M., Caixeta Filho, J. V. & Rodrigues, L. Study of optimal locations for new sugarcane mills in brazil: Application of a minlp network equilibrium model. *Biomass and Bioenergy* **127**, 105249 (2019).

18. EPE. Cenários de oferta de etanol e demanda de ciclo otto 2020-2030. Tech. Rep., Empresa de Pesquisa Energética (2019).

19. Equinor. Apodi solar plant in commercial operation (2018). URL https://www.equinor.com/en/news/apodi-solar-plant-in-commercial-operation.html. [Online; accessed 2020-10-22].

20. Hernandez, R. R., Hoffacker, M. K. & Field, C. B. Land-use efficiency of big solar. *Environmental Science & Technology* **48**, 1315–1323 (2014). Publisher: American Chemical Society.

21. Denholm, P. & Margolis, R. M. Land-use requirements and the per-capita solar footprint for photovoltaic generation in the united states. *Energy Policy* **36**, 3531–3543 (2008).

22. Ong, S., Campbell, C., Denholm, P., Margolis, R. & Heath, G. Land-use requirements for solar power plants in the united states. Tech. Rep., NREL (2013). URL http://www.osti.gov/servlets/purl/1086349/. DOI: 10.2172/1086349.

23. Wirth, H. Recent facts about photovoltaics in germany. Tech. Rep., Fraunhofer ISE (2020). URL https://www.pv-fakten.de.

24. Atikol, U., Abbasoglu, S. & Nowzari, R. A feasibility integrated approach in the promotion of solar house design. *International Journal of Energy Research* **37**, 378–388 (2013).